High intracellular chloride delays the activation of the volume-sensitive chloride conductance in mouse L-fibroblasts

P. Doroshenko

Loeb Research Institute, University of Ottawa, Ottawa, Canada

(Received 13 July 1998; accepted after revision 8 October 1998)

1. The relationship between cell volume and volume-sensitive Cl^- conductance during hyposmotic cell swelling of patched cells and the effects of intracellular chloride on the conductance have been studied in mouse L-fibroblasts. To this end, swelling-activated current and cell volume were measured simultaneously in cells dialysed with low-Cl^- (16 mM) or high-Cl^- (130 mM) solutions using the whole-cell patch-clamp technique and videomicroscopy.

2. The increase in cell volume of patched cells and the volume-sensitive conductance saturated during a 4–5 min exposure to mildly hyposmotic solutions (15–20% less than isosmotic). The swelling of patched cells varied considerably and was greater than the swelling of intact cells. No correlation between the maximal values of the volume-sensitive conductance and the maximal volumes of swollen cells was evident for cells dialysed with the low-Cl^- solutions.

3. The amplitude of the volume-sensitive conductance decreased with a reduction in either extracellular or intracellular Cl^- concentration; the size of the maximal conductance was not modulated by intracellular Cl^- ions.

4. The activation of the volume-sensitive conductance was slower in high-Cl^- cells than in low-Cl^- cells whether it was induced by hypotonic cell swelling or by cell inflation; in low-Cl^- cells the conductance saturated before the cell volume had reached its maximal value.

5. It is concluded that in patched cells an increase in cell volume triggers activation of the volume-sensitive Cl^- conductance but does not determine its amplitude and that the rate of activation of the conductance is affected by the intracellular Cl^- concentration.

Volume-sensitive Cl^- currents activated by cell swelling have been described in many cell types (reviewed by Hoffmann & Simonsen, 1989; Nilius *et al.* 1996). The mechanisms whereby an increase in cell volume is transduced into opening of volume-sensitive Cl^- channels have yet to be established. Significant progress in our understanding of the transduction process (reviewed by Hoffmann & Dunham, 1995; Strange *et al.* 1996; Okada, 1997) can be justifiably attributed to the use of the whole-cell patch-clamp technique (Hamill *et al.* 1981) which allows the composition of the intracellular milieu to be manipulated. On the other hand, the technique also introduced new experimental variables. One of them is that intracellularly dialysed cells exposed to a hyposmotic medium swell differently from intact cells. In the whole-cell mode, the cell interior is physically connected to an infinite volume of the patch pipette. Consequently, hyposmotic swelling of a patched cell cannot bring about the equilibration of the extracellular and intracellular osmolalities and thus limit itself (see discussion by Ross *et al.* 1994).

Another consequence of the whole-cell recording mode is an inevitable disruption of physiological intracellular concentrations of mobile electrolytes, mostly Cl^- and K^+ ions which are the major ionic constituents of the cell cytosol. Especially significant may be the changes in $[Cl^-]_i$ because in intact cells it is likely to be low, ~10 mM (e.g. in mammalian neurones; Ebihara *et al.* 1995), while patch pipette solutions often contain more than 100 mM Cl^-. Cytosolic Cl^- has been reported to affect various cellular functions, e.g. the agonist-induced responses (Nakajima *et al.* 1992; Robertson & Foskett, 1994; Lenz *et al.* 1997) and, in particular, the activity of the cystic fibrosis transmembrane conductance regulator (CFTR) Cl^- channels (Wang *et al.* 1993) and volume-sensitive organic osmolyte/anion (VSOAC) channels (Jackson *et al.* 1996).

The goals of the present study were to investigate the relationship between cell volume and volume-sensitive Cl^- conductance during hyposmotic swelling of patched cells, as well as possible regulatory effects of cytosolic chloride on the volume-sensitive Cl^- channels in mouse fibroblasts.

METHODS

The investigations were carried out on mouse L-fibroblasts (LM TK- cell line, American Type Culture Collection No. CCL-1.3). Cell monolayers were cultured at 37 °C in DMEM/F12 medium mixture supplemented with 10 % fetal bovine serum and antibiotics (GibcoBRL Life Technologies, Burlington, Ontario, Canada). Before the experiments, dissociated cells were plated on 12 mm diameter glass coverslips and grown for 24–48 h. For electrical recording, coverslips were placed in a recording chamber mounted on the stage of an inverted microscope (Axiovert 100, Carl Zeiss, Germany). The ~500 μl chamber was continuously perfused with the control bath solution using a conventional gravity-fed flow system (~1 ml min^{-1}). Whole-cell patch-clamp recordings were performed using the Axopatch 200A amplifier (Axon Instruments). A Digidata 1200 interface board, installed in a Compaq ProLinea 486 computer, and pCLAMP software (version 6.0.2, Axon Instruments) were used to generate voltage-clamp command voltages and acquire data (50 ms sampling interval). Cell capacitance and series resistance, measured at the end of the recording periods using the compensatory circuitry of the patch-clamp amplifier, had mean values of 14·1 ± 0·4 pF and 6·1 ± 0·2 MΩ ($n = 131$), respectively. Membrane conductance, defined as the slope of the I–V characteristics at the reversal potential, was measured every 30 s by ramping the membrane voltage from +60 to −60 mV (over 2·5 s) relative to a chosen holding potential. The generated I–V curves were fitted with a second order polynomial and the membrane conductance at different membrane potentials was calculated using the fit parameters. To quantify the time course of changes in the membrane conductance or cell volume, the respective experimental data were fitted to a Boltzmann sigmoidal (S-shaped) curve $Y(t) = Y_0 + (Y_{max} - Y_0)/(1 + \exp((T_{50} - t)/L))$. In this equation Y_0 and Y_{max} are minimal and maximal values of the function, respectively. T_{50} is the half-activation time. L is the slope parameter, which is related to the maximal rate of the function change by the equation $(dY/dt)_{max} = Y_{max}/(4L)$. In inflated cells the time course of the membrane conductance was fitted to a one-phase exponential association curve $Y(t) = Y_{max}(1 - \exp(-kt))$, where k is a rate constant related to the half-activation time by the equation $T_{50} = 0{\cdot}69/k$. All fits were performed with Prism 2.01 software (GraphPad Software, San Diego, CA, USA).

The cells were normally bathed in a solution containing (mM): 130 NaCl, 5 $CaCl_2$, 2 $MgCl_2$, 2·8 KCl and 10 Hepes; with the pH adjusted to 7·4 with Tris-OH and the osmolality adjusted to 300 mosmol kg^{-1} with mannitol. The hyposmotic solution contained (mM): 107 NaCl, 5 $CaCl_2$, 2 $MgCl_2$, 2·8 KCl, 10 Hepes; pH 7·4 with Tris-OH and mannitol to obtain an osmolality of 240 mosmol kg^{-1} (−20 % hyposmotic) or 255 mosmol kg^{-1} (−15 % hyposmotic). The pipette solutions contained (mM): (low-Cl^-) 127 potassium aspartate (or 120 mM potassium gluconate, or 120 mM potassium glutamate), 16 KCl, 2 $MgSO_4$, 2 ATP, 1 EGTA, 20 Hepes; pH 7·25 with Tris-OH (285 mosmol kg^{-1}); or (high-Cl^-) 130 KCl, 2 $MgSO_4$, 2 ATP, 1 EGTA, 20 Hepes; pH 7·25 with Tris-OH (285 mosmol kg^{-1}). In initial experiments (Fig. 1*A* and *B*), the hyposmotic extracellular solution contained (mM): 65 NaCl, 1·8 $CaCl_2$, 1 $MgCl_2$, 2·8 KCl, 10 Hepes; pH 7·4 with Tris-OH, 240 mosmol kg^{-1} with mannitol; and the pipette solution contained (mM): 140 CsCl, 2 $MgSO_4$, 2 ATP, 1 EGTA, 20 Hepes; pH 7·2 with Tris-OH, 285 mosmol kg^{-1}. The osmolality of solutions was measured with a micro-osmometer model 3MO (Advanced Instruments, Needham Heights, MA, USA).

An increase in volume of patched cells was induced by application of hyposmotic solutions using an application pipette (~50 μm tip) whose tip was positioned ~250 μm from the patched cell. A gravity-fed solution flow through the application pipette was gated by two electronically controlled valves (General Valve, Fairfield, NJ, USA). In other experiments, instead of hyposmotic swelling, an increase in cell volume was induced by short (1–3 s) pulses of positive pressure (1·3–2·6 kPa) applied through the patch pipette.

Cell volume measurements were performed with a video imaging system consisting of a CCD video camera (Cohu, model 4915-2000, San Diego, CA, USA) attached to an Axioscope microscope equipped with differential interference contrast (DIC) optics and a Zeiss ×40 (NA 0·65) objective lens. The camera output was fed into a frame grabber DT3155 (Data Translation, Marlboro, MA, USA) installed into a 166 MHz Pentium computer. Cell images were collected every 30 s during 5 min-long recording periods and analysed off-line using the UTHSCSA ImageTool v. 1.28 program (developed at the University of Texas Health Science Center at San Antonio, Texas and available from the Internet by anonymous FTP from maxrad6.uthscsa.edu). Cell images were displayed on a 17 in colour monitor and the cross-sectional area (CSA) of the soma of single cells was measured by tracing cell borders with a computer-generated cursor. The relative cell volume changes (V/V_o) were calculated using the equation $V/V_o = (\text{test CSA}/\text{control CSA})^{3/2}$ (see Churchwell *et al.* 1996).

Experiments were conducted at room temperature (21–23 °C). The results were corrected for liquid junction potentials arising between the pipette or the bath electrode and the various extracellular solutions. Junction potentials were measured separately against a 3 M KCl-filled reference pipette (Neher, 1992). Unless otherwise indicated, results are presented as means ± S.E.M. Statistical comparisons were performed using ANOVA or Student's t test (Prism 2.01). A P value $< 0{\cdot}05$ was defined as being statistically significant.

RESULTS

Hyposmotic swelling and swelling-activated membrane conductance in patched fibroblasts

Immediately after establishment of the whole-cell patch-clamp mode, membrane conductance measured on average 0·95 ± 0·07 nS ($n = 119$). In the absence of changes in osmolality of the extracellular medium, conductance remained low, increasing only slightly during the entire recording period. In general, such spontaneous increases in membrane conductance were smaller in cells dialysed with low-Cl^- pipette solutions than in cells dialysed with high-Cl^- solutions. In a group of control cells ($n = 5$) dialysed with a high-Cl^- (140 mM CsCl) solution, where the membrane conductance was monitored during the entire recording period, the spontaneous conductance increase had a mean value of 3·3 ± 0·8 nS (Fig. 1*A*, open symbols). The I–V characteristics of the spontaneous membrane current showed a slight outward rectification and crossed the voltage axis in the vicinity of 0 mV. Often, such spontaneous increases in the membrane conductance were accompanied by small visible increases in cell volume (swelling or cell blebbing).

Cell swelling caused by a decrease in the extracellular osmolality (by 20 %, from 300 to 240 mosmol kg^{-1}) was accompanied by a much larger increase in membrane conductance. This increase in membrane conductance continued for some time during hyposmotic application and eventually levelled off (Fig. 1*A*, filled symbols). This

saturation of the conductance increase allowed the use of an S-shaped Boltzmann curve to fit the time course of the conductance activation (curve 2 in Fig. 1*A*). The half-maximal activation was reached about 2 min after the hyposmotic application began. As can be seen in Fig. 1*A*, a 4–5 min exposure to hyposmotic solution was sufficiently long to fully activate the volume-sensitive membrane conductance. The maximal mean value of the swelling-activated conductance (see below) in these high-Cl^- cells was $24{\cdot}2 \pm 0{\cdot}4$ nS ($n = 11$). The *I–V* characteristics of the swelling-induced membrane current (Fig. 1*B*, curve 2) displayed a moderate outward rectification, with the conductance measured at $V_m = +50$ mV (27·6 nS) being twice that measured at $V_m = -50$ mV (13·9 nS). For a more accurate comparison of the volume-sensitive conductance measured under different ionic conditions, the conductance values presented below were calculated at the reversal potential for the swelling-induced current (see Methods). In the above experiments, the reversal potential of the current, $10{\cdot}3 \pm 0{\cdot}5$ mV ($n = 11$), approached the equilibrium potential for chloride, $E_{Cl} = +15$ mV (with 74 mM Cl^- in the hyposmotic solution), suggesting that Cl^- ions contributed most to the swelling-induced current.

When applying a hyposmotic solution to swell cells in the whole-cell mode, it was noticed that patched cells swelled more dramatically than their intact neighbours. Figure 1*C* compares hyposmotic swelling of intact and patched cells from the same coverslips during application of the 20% hyposmotic solution. Each of the measured intact cells was located on a coverslip in the vicinity of the patched cell and thus was exposed to hyposmotic shock simultaneously with its patched counterpart. By the end of a 4 min hyposmotic application the intact cells swelled by $23 \pm 2\%$ ($n = 16$), approaching the expected increase in volume of an ideal osmometer (25%). The increase in cell volume occurred in two phases. Most of the increase in cell volume, 13·6% or about 2/3 of the total increase, occurred during the first minute of hyposmotic exposure, at the rate of 18% min^{-1} (Fig. 1*C*, open symbols). The later phase, between 1·25 and 4·25 min, accounted for an additional 9% increase in cell volume at the rate of 3% min^{-1}. In contrast, during the same period the volume of the patched cells had increased by $150 \pm 23\%$ ($n = 10$), at the maximal rate of 50% min^{-1}, with distinct slowing by the end of the application (Fig. 1*C*, filled symbols). Such a large increase in volume of patched cells, more than 6 times that observed in intact cells,

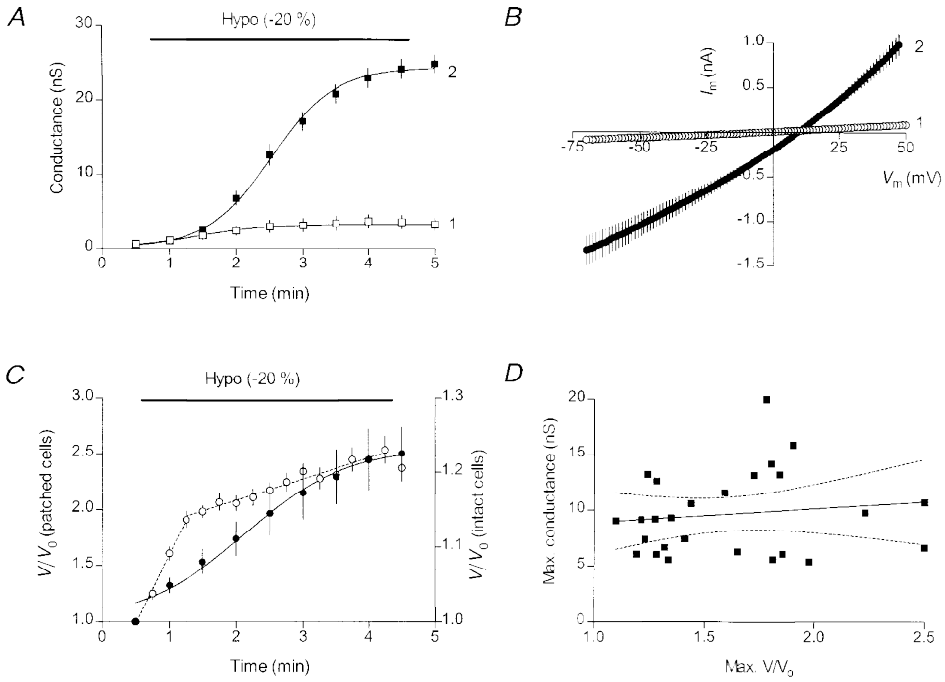

Figure 1. Hyposmotic swelling-induced current in L-fibroblasts

A, time course of the membrane conductance change in cells dialysed with the high-Cl^- (140 mM CsCl) solution in the absence of hyposmotic challenge (□, $n = 5$) and during application of the hyposmotic (240 mosmol kg^{-1}) solution (■, $n = 11$). *B*, mean *I–V* characteristics for the hyposmotically swollen cells ($n = 11$) measured at the break-in (curve 1) and at 4·5 min (curve 2). *C*, comparison of hyposmotic swelling of intact and patched cells. ○, data for intact cells (the right *Y*-axis scale), $n = 16$. The regression lines were drawn with a slope of 18·5% min^{-1} for the 0·5–1·25 min interval and 2·9% min^{-1} for the 1·25–4·25 min interval. ●, data for patched cells (the left *Y*-axis scale), $n = 10$. The cells were dialysed with a low-Cl^-, gluconate-substituted pipette solution. *D*, correlation between the maximal swollen volumes and the swelling-induced conductances in cells dialysed with low-Cl^- solutions ($n = 26$) and swollen by a 15% decrease in the extracellular osmolality (to 255 mosmol kg^{-1}). The slope of the regression line is $1{\cdot}27 \pm 1{\cdot}90$ ($P = 0{\cdot}510$, $F = 0{\cdot}448$). Dotted lines show the 95% confidence intervals. Holding potential was −37 mV.

demonstrates that the magnitude of hyposmotic shift used to swell cells in whole-cell experiments was not the decisive factor in determining the extent of cell swelling.

Furthermore, in similar experiments carried out over an extended period of time the observed increases in volume of patched cells swollen by the same hyposmotic shift varied considerably. In Fig. 1*D* the maximal values of the volume-sensitive conductance measured in swollen cells were plotted against their maximal volumes. The cells included in the analysis ($n = 26$) were dialysed with low-Cl^- pipette solutions and were swollen by 15% reduction in the extracellular osmolality (from 300 to 255 mosmol kg^{-1}). Although the hyposmotic shock was the same in each experiment, increases in volume of these patched cells ranging from 20 to 150% were observed. Obviously, some other, as yet unidentified parameter(s) of the cell–patch pipette system (e.g. access resistance) may affect swelling of patched cells. The corresponding conductance values were less scattered. Although they tended to increase as the cells swelled more, especially for smaller increases in cell volume, no correlation between the two parameters was evident for the entire group. The slope of the linear regression line drawn through the data points was not significantly different from zero ($P = 0{\cdot}510$).

The effects of lowering the intracellular Cl^- concentration on the amplitude of the volume-sensitive conductance

In agreement with the predominantly chloride nature of the swelling-induced current, a decrease in the intracellular chloride concentration, $[Cl^-]_i$, shifted the reversal potential to more negative membrane voltages. In experiments presented in Fig. 2, cells from the same passage, randomly dialysed either with the low-Cl^- ($[Cl^-]_i = 16$ mM Cl^-) or with the high-Cl^- ($[Cl^-]_i = 130$ mM Cl^-) pipette solution, were swollen by exposure to the same hyposmotic solution (240 mosmol kg^{-1}, $[Cl^-]_o = 124$ mM Cl^-). Figure 2*A* shows the *I–V* characteristics of the swelling-induced current in the high-Cl^- cells at the end of the 4·5 min exposure. The reversal potential for the current was $+2{\cdot}8 \pm 0{\cdot}6$ mV ($n = 7$), with $E_{Cl} = 3$ mV. In cells dialysed with the low-Cl^- solution, the swelling-induced current reversed at $-37{\cdot}0 \pm 1{\cdot}6$ mV (Fig. 2*B*). The deviation of the low-Cl^- reversal potential from $E_{Cl} = -52$ mV can be accounted for by assuming that aspartate, used as a Cl^- substitute in the pipette solution, can permeate the volume-sensitive channels with aspartate permeablility (P_{asp}) ~0·1 P_{Cl}.

Comparison of the *I–V* relationships for the high-Cl^- and low-Cl^- cells (Fig. 2*A*) shows that they differed most at negative membrane voltages (between −50 and −75 mV),

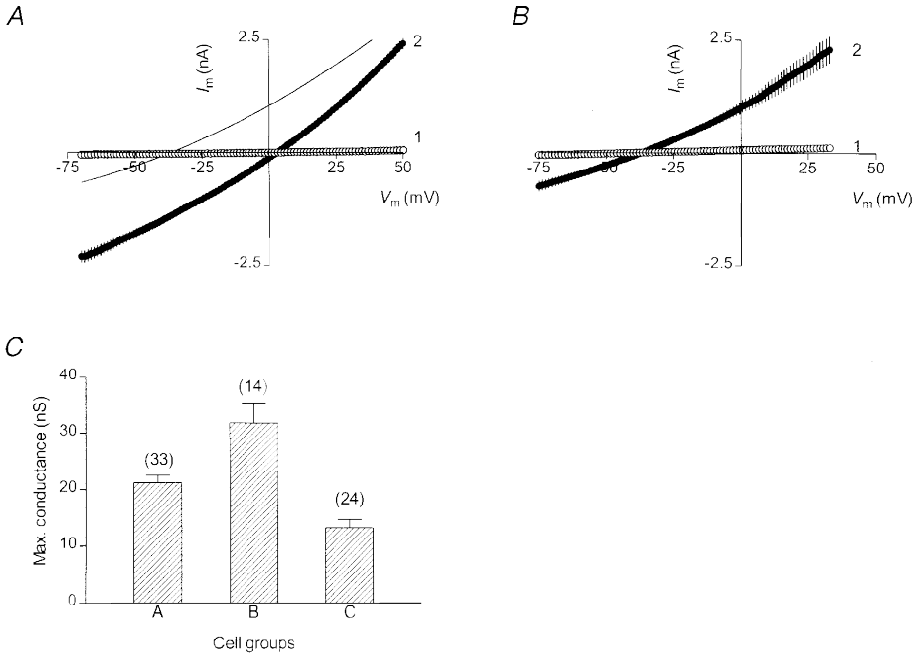

Figure 2. Chloride dependence of the swelling-induced current

A, mean ($n = 7$) *I–V* characteristics of the swelling-induced current (curve 2) in cells dialysed with the high-Cl^- (130 mM KCl) pipette solution. The extracellular hyposmotic solution (240 mosmol kg^{-1}) contained 124 mM Cl^-. Holding potential was 3 mV. Curve 1 in this (and the next) panel shows the pre-swelling *I–V* characteristics. The thin line shows a 2nd order polynomial fit to the *I–V* curve for the low-Cl^- cells (from panel *B*) for comparison. *B*, mean ($n = 6$) *I–V* characteristics of the swelling-induced current (curve 2) in cells dialysed with the low-Cl^- (16 mM Cl^-, aspartate-substituted) solution. Holding potential was −37 mV. *C*, comparison of the maximal values of the swelling-induced conductance at three different transmembrane Cl^- gradients (see the text). Number of cells in each group is shown above the corresponding bars.

whereas at high positive voltages (+25 to +50 mV) the respective membrane currents were almost equal. These changes are consistent with an assumption that in the low-Cl^- cells the volume-sensitive Cl^- conductance was smaller than in the high-Cl^- cells; and this was because of a smaller efflux of intracellular Cl^- ions, which creates the inward component of the transmembrane current and dominates the total membrane current at negative voltages. The influx of extracellular Cl^- ions, which creates the outward component of the current and contributes mostly at positive membrane voltages, did not change significantly because the $[Cl^-]_o$ was the same for the two cell groups. In other words, the observed differences between the two *I–V* curves indicate that the maximal size of the volume-sensitive conductance is not modulated by the intracellular Cl^- ions.

The amplitude of the swelling-induced conductance increased with a rise in either extracellular or intracellular Cl^- concentration. The maximal values of the resulting conductance (G_{max}) measured at three different transmembrane Cl^- gradients are shown in Fig. 2*C*. In group A, with $[Cl^-]_o/[Cl^-]_i = 74$ mM/140 mM, G_{max} had a mean value of $21{\cdot}2 \pm 1{\cdot}3$ nS ($n = 33$). Increasing $[Cl^-]_o$ to 124 mM (with $[Cl^-]_i = 130$ mM) gave a higher G_{max} of $31{\cdot}9 \pm 3{\cdot}4$ nS (group B, $n = 14$), whereas decreasing $[Cl^-]_i$ to 16 mM but maintaining $[Cl^-]_o$ at 124 mM resulted in a lower G_{max} of $13{\cdot}3 \pm 1{\cdot}5$ nS ($n = 24$). The differences between the mean conductance values were highly significant (ANOVA, $P < 0{\cdot}0001$, $F = 19{\cdot}69$).

Kinetics of cell volume increase and activation of the volume-sensitive conductance in patched cells

Whilst a decrease in the intracellular concentration of Cl^- ions affected the maximal values of the swelling-induced conductance in a manner consistent with their role as the predominant charge carriers, the effects on the time course of cell swelling and the conductance activation were more complex. Figure 3 shows the results of a series of similar experiments carried out on several cells from the same coverslip. Each cell was swollen by exposure to the same hyposmotic solution (255 mosmol kg^{-1}) but was dialysed with either low-Cl^- (gluconate-substituted solution) or high-Cl^- pipette solutions. The use of cells from the same coverslip was intended to reduce any variation in the experimental conditions and, therefore, to enhance the comparison between these cells. The holding potentials for the low-Cl^-

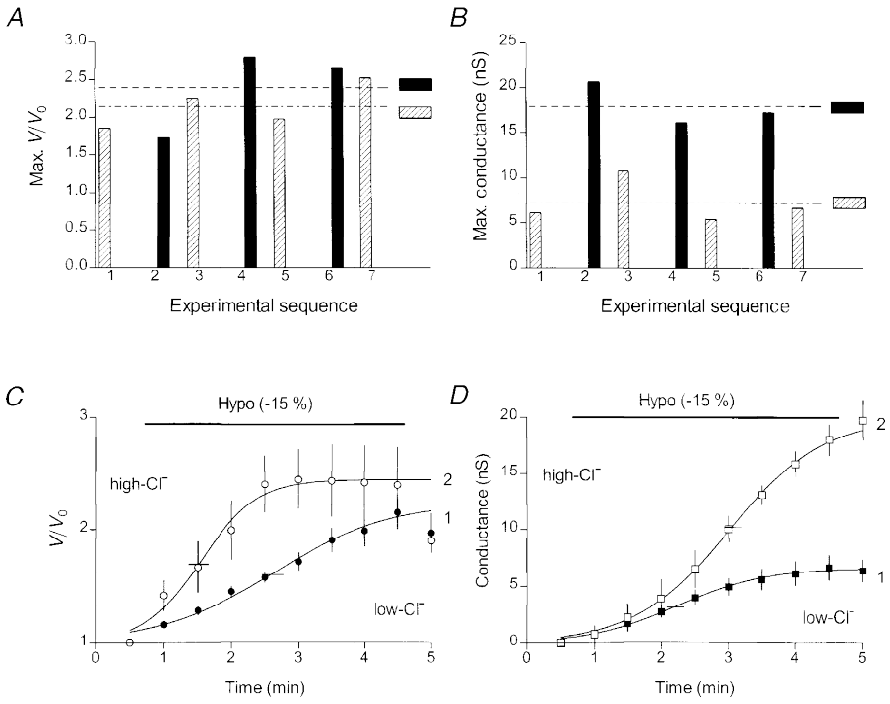

Figure 3. Kinetics of hyposmotic cell swelling and the swelling-induced conductance in patched cells at two intracellular Cl^- concentrations

A, comparison of maximal volumes of swollen patched cells from the same coverslip dialysed with either the low-Cl^- (gluconate-substituted pipette solution, ▨) or high-Cl^- solution (■) during application of the 255 mosmol kg^{-1} (−15%) hyposmotic solution. The mean volumes of swollen cells in each group are shown by the horizontal interrupted lines. *B*, comparison of maximal swelling-induced conductances in the same cells. The interrupted lines show the mean conductances in each cell group. *C*, time course of volume changes in the low-Cl^- (●, $n = 4$) and the high-Cl^- (○, $n = 3$) cells. Short horizontal lines (here and in panel *D*) cross the fitted curves at their mid-points. *D*, time course of the swelling-induced conductance in the low-Cl^- (■) and the high-Cl^- (□) cells. Here and in the following figures, the pre-swelling conductance value has been subtracted from all conductance values.

and high-Cl^- cells were different and kept at their respective reversal potential for the swelling-activated current: −37 mV for the low-Cl^- cells and +3 mV for the high-Cl^- cells. The change in the holding potential did not affect either cell swelling or the volume-sensitive Cl^- current (data not shown). As expected, the maximal volumes of the swollen cells in the two groups were not significantly different ($P = 0{\cdot}497$); $240 \pm 34\%$ ($n = 3$) for the high-Cl^- cells (filled bars in Fig. 3*A*) and $215 \pm 15\%$ ($n = 4$) for the low-Cl^- cells (hatched bars in Fig. 3*A*). Also in agreement with the previous results, the maximal Cl^- conductances in these two cell groups were different ($P = 0{\cdot}002$): $7{\cdot}2 \pm 1{\cdot}2$ nS ($n = 4$) in the low-Cl^- cells and $18{\cdot}0 \pm 1{\cdot}4$ nS ($n = 3$) in the high-Cl^- cells.

Rather unexpected was the finding that the time course of swelling was different for the low-Cl^- and the high-Cl^- cells. During hyposmotic exposure cell volume in the high-Cl^- cells (open symbols, curve 2 in Fig. 3*C*) increased faster and saturated earlier than in the low-Cl^- cells (filled symbols, curve 1 in Fig. 3*C*). The respective times for a half-maximal increase in cell volume ($T_{50,V}$), $1{\cdot}1 \pm 0{\cdot}2$ min ($n = 3$) in the high-Cl^- cells and $2{\cdot}1 \pm 0{\cdot}2$ min ($n = 4$) in the low-Cl^- cells, were significantly different ($P = 0{\cdot}021$). On the other hand, volume-sensitive conductance developed faster in the low-Cl^- cells (filled symbols, curve 1 in Fig. 3*D*) than in the high-Cl^- cells (open symbols, curve 2 in Fig. 3*D*). Half-maximal activation of the conductance ($T_{50,G}$) in the low-Cl^- cells was reached in $1{\cdot}7 \pm 0{\cdot}1$ min ($n = 4$) as compared with $2{\cdot}2 \pm 0{\cdot}3$ min ($n = 3$) in the high-Cl^- cells. Consequently, in the high-Cl^- cells, the increase in the volume-sensitive conductance was delayed in relation to the increase in cell volume. On the other hand, in the low-Cl^- cells the conductance saturated before the increase in cell volume had reached its maximal values.

These findings were reinforced when the analysis was extended to include additional high-Cl^- cells from other experiments and low-Cl^- cells dialysed with aspartate-substituted and glutamate-substituted pipette solutions. In Fig. 4 the time course of cell swelling and activation of the swelling-induced conductance are compared on the same graph for each of the four cell groups. To make such comparisons possible, the mean data for the increase in cell volume, $\Delta(V/V_0)$, and the conductances (similar to those shown in Fig. 3*C* and *D*) were normalized to their respective maximal mean values in each group of cells. For the group of high-Cl^- cells (Fig. 4*A*), $T_{50,V}$ was $1{\cdot}0 \pm 0{\cdot}1$ min ($n = 7$) and $T_{50,G}$ was $2{\cdot}2 \pm 0{\cdot}1$ min ($n = 7$). The times for half-maximal increase in cell volume or in conductance were similar in each of the three low-Cl^- cell groups. $T_{50,V}$ was $1{\cdot}8 \pm 0{\cdot}1$ min for aspartate-substituted low-Cl^- solution ($n = 18$, Fig. 4*B*), $1{\cdot}8 \pm 0{\cdot}1$ min for gluconate-substituted solution ($n = 7$, Fig. 4*C*) and $2{\cdot}0 \pm 0{\cdot}1$ min for glutamate-substituted solution ($n = 6$, Fig. 4*D*). $T_{50,G}$ was $1{\cdot}0 \pm 0{\cdot}1$ min ($n = 18$), $1{\cdot}2 \pm 0{\cdot}1$ min ($n = 13$), and $1{\cdot}2 \pm 0{\cdot}1$ min ($n = 8$)

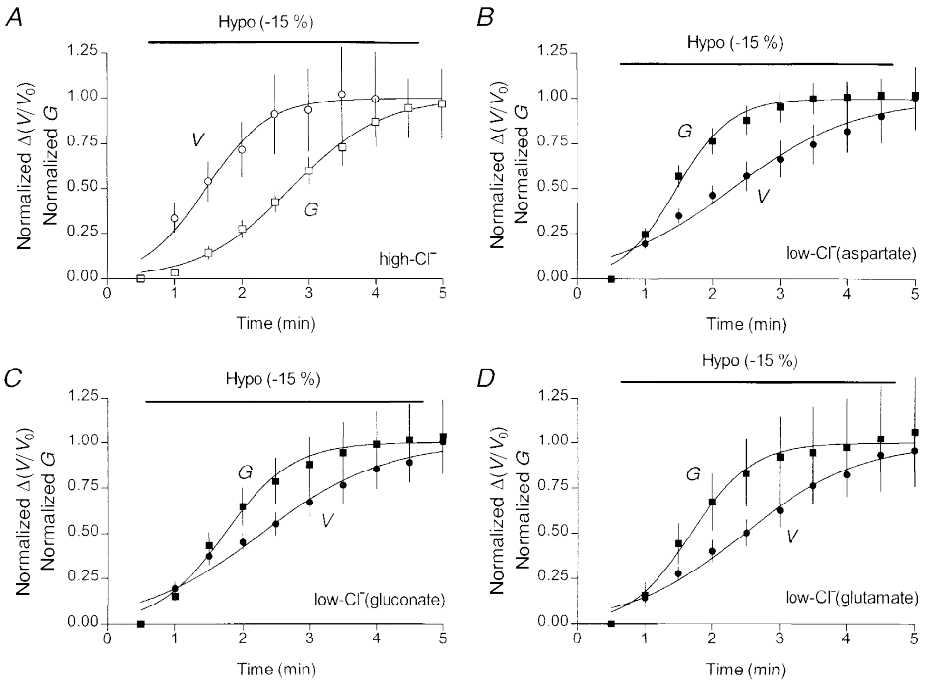

Figure 4. Comparison of the time courses of cell swelling and the activation of the volume-sensitive conductance in cells dialysed with different solutions

Each panel compares the time courses of cell swelling (V) and activation of the volume-sensitive Cl^- conductance (G) within one cell group. *A*, high-Cl^- cells ($n = 7$). *B*, low-Cl^- cells with aspartate as a Cl^- substitute ($n = 18$). *C*, low-Cl^- cells with gluconate as a Cl^- substitute ($n = 7$ for volume and $n = 13$ for conductance data). *D*, low-Cl^- cells with glutamate as a Cl^- substitute ($n = 6$ for volume and $n = 8$ for conductance data).

for the three solutions, respectively. The almost 2-fold difference between the $T_{50,G}$ values for the low-Cl^- and high-Cl^- cells was significant ($P < 0{\cdot}01$) for each of the low-Cl^- cell groups.

Time course of activation of the volume-sensitive conductance in inflated cells

In hypotonically swollen cells the time course of activation of the volume-sensitive membrane conductance may be complicated by changes in cell volume (see Fig. 4). To avoid, or at least to lessen such a dependence, the kinetics of the conductance increase was studied in cells whose volume was increased by inflation through the patch pipette. Chloride currents activated by cell inflation have been shown previously to be indistinguishable from the osmotic swelling-induced volume-sensitive Cl^- current in bovine chromaffin cells (Doroshenko & Neher, 1992), in rabbit supraventricular cells (Hagiwara *et al.* 1992), and in dog atrial myocytes (Du & Sorota, 1997). During inflation with a short pulse of positive pressure (see Methods) cell volume increased very rapidly and reached its maximal value within a few seconds (not shown). Cells from the same passage were bathed in a standard solution (300 mosmol kg^{-1}) and dialysed with either low-Cl^- (aspartate-substituted) or high-Cl^- pipette solutions (Fig. 5). A single short pressure pulse was applied through the suction outlet of the patch pipette $\geqslant 1$ min after establishment of the whole-cell mode, immediately after the control measurement of the membrane conductance (time zero in Fig. 5). At the time of the subsequent conductance measurement (at 0·5 min) the average volumes of inflated cells in the two groups were not significantly different from each other ($P = 0{\cdot}146$): $184 \pm 13\,\%$ in the low-Cl^- cells ($n = 6$) and $158 \pm 10\,\%$ in the high-Cl^- cells ($n = 6$). As in hyposmotically swollen cells, the maximal inflation-induced conductance was significantly smaller ($P = 0{\cdot}016$) in the low-Cl^- cells than in the high-Cl^- cells: $7{\cdot}2 \pm 1{\cdot}7$ nS (at 2·5 min, $n = 6$) and $22{\cdot}5 \pm 5{\cdot}0$ nS (at 3 min, $n = 6$), respectively. In cells from both groups the volume-sensitive conductance reached maximal levels in 2·5–3·5 min, but at different rates. The time course of conductance activation in individual cells is shown in Fig. 5*A* (low-Cl^- cells) and Fig. 5*B* (high-Cl^- cells). It was obvious that volume-sensitive conductance reached its maximal values much faster in the low-Cl^- cells than in the high-Cl^- cells. The experimental data points during the first 3 min were fitted to the one-phase exponential association curves; in inflated cells, especially in those dialysed with the low-Cl^- solution, these curves had a better fit to the experimental data than the Boltzmann S-shaped curves used to describe the time course of conductance activation in the hypotonically swollen cells. The half-activation times for the conductance estimated from the fits were significantly different ($P = 0{\cdot}003$): $0{\cdot}4 \pm 0{\cdot}1$ min ($n = 6$) for the low-Cl^- cells and $1{\cdot}1 \pm 0{\cdot}2$ min ($n = 6$) for the high-Cl^- cells. This result was independent of the fitting method used. The Boltzmann fit also produced a significant difference ($P = 0{\cdot}02$) between the half-activation times for the two cell groups: $0{\cdot}6 \pm 0{\cdot}1$ min ($n = 6$) for the low-Cl^- cells and $1{\cdot}0 \pm 0{\cdot}1$ min ($n = 6$) for the high-Cl^- cells. However, in this instance the mean values were closer to each other due to a poorer fitting of the low-Cl^- data points with the S-shaped Boltzmann curves.

DISCUSSION

Hyposmotic swelling of intracellularly dialysed cells

Intracellular dialysis, which is an essential component of the whole-cell patch-clamp technique and provides for a direct contact between the cytoplasm and patch pipette-filling solution, significantly changes conditions for hyposmotic cell swelling. In intact cells, hyposmotic cell swelling leads to dilution of the intracellular milieu which decreases the transmembrane osmotic gradient and thereby limits cell swelling. In a patched cell connected to a patch pipette of virtually infinite volume the swelling conditions are fundamentally different. Osmotically driven transmembrane influx of water cannot significantly change the osmolality of the intracellular milieu any longer and the transmembrane osmotic gradient will exist as long as the extracellular

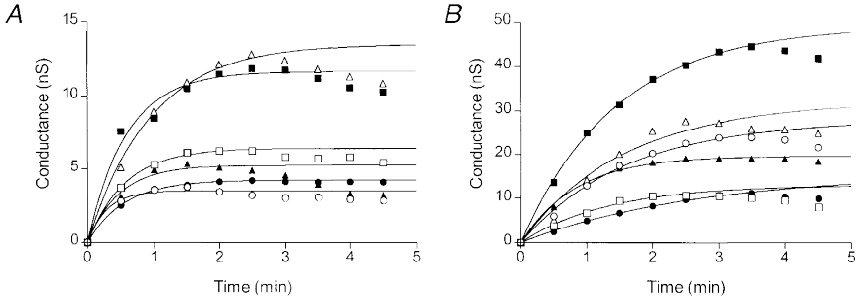

Figure 5. Kinetics of inflation-induced Cl^- conductance at two intracellular Cl^- concentrations

Time courses of the inflation-induced Cl^- conductance in individual low-Cl^- (*A*) or high-Cl^- (*B*) cells. Each cell was inflated immediately after the first measurement of the conductance (time zero in each plot). The lines are the single-phase exponential association curves fitted to the conductance values in individual cells within the first 3 min. The individual half-activation times are 0·20 (○), 0·39 (□), 0·65 (△), 0·38 (●), 0·40 (■) and 0·33 min (▲) for the low-Cl^- cells and 1·13 (○), 0·93 (□), 1·10 (△), 1·87 (●), 1·01 (■) and 0·59 min (▲) for the high-Cl^- cells.

solution remains hyposmotic. The patched cell will continue to swell because there is no osmotic mechanism in place to limit the swelling (see discussion by Ross *et al.* 1994). Theoretically, a small physiologically 'reasonable' hyposmotic shift may result in an 'unreasonably' large swelling of a patched cell. Such an excessive swelling during intracellular dialysis with hypertonic solutions has been observed in patched neutrophils (Stoddard *et al.* 1993), lymphocytes (Ross *et al.* 1994) and epidermoid KB cells (Miwa *et al.* 1997).

The observations reported here are in agreement with this analysis. When challenged with a 20% decrease in the bath osmolality (from 300 to 240 mosmol kg^{-1}), intact cells swelled by ~23% (Fig. 1*C*). Similarly, near-perfect osmometric behaviour has been reported for intact growth hormone-producing rat type II somatotrophs (Engstrom & Savendahl, 1995), N1E-115 neuroblastoma cells (Crowe *et al.* 1995), and for insect Sf-9 and pig kidney epithelial LLC-PK1 cells (Farinas *et al.* 1995). On the contrary, hyposmotic swelling of patched cells was much larger (Fig. 1*C*) and more variable. In a group of low-Cl^- cells the same 15% hyposmotic shift in the extracellular osmolality produced increases in cell volume that differed 2-fold (Fig. 1*D*). The mechanisms that limit hyposmotic swelling of patched cells remain unclear but participation of non-osmotic factors (e.g. mechanical forces of the plasma membrane/cytoskeleton; Ross *et al.* 1994) cannot be excluded. It is also plausible that, because the intracellular volume of patched cells is physically connected to a much larger volume of the cell–patch pipette system, other parameters of the system (e.g. access resistance of the patch pipette or the hydrostatic pressure of the pipette-filling solution) contribute to this process.

Another major consequence of disruption of the membrane patch and attainment of whole-cell recording is the so-called 'wash-out' of mobile components of the cytosol. A restricted diffusion of large cytosolic constituents has been suggested to cause spontaneous cell swelling (Worrell *et al.* 1989; Kubo & Okada, 1992) and activation of a membrane conductance under isosmotic recording conditions in human airway epithelial cells (McCann *et al.* 1989), T84 cells (Worrell *et al.* 1989) and human neutrophils (Stoddard *et al.* 1993). The small increase in membrane conductance observed in the control cells (Fig. 1*A*, curve 1) is likely to be such a spontaneously activated volume-sensitive conductance.

Volume-sensitive Cl^- conductance in L-fibroblasts

Although the presence of the swelling-activated current in L-fibroblasts was reported earlier (Nilius *et al.* 1994), it has not been studied in detail. The conductance activated during hyposmotic swelling of fibroblasts displayed a characteristic delay similar to that reported earlier in various cell types such as lymphocytes (Lewis *et al.* 1993; Ross *et al.* 1994), chromaffin cells (Doroshenko & Neher, 1992) and cardiac myocytes (Sorota, 1992; Sakaguchi *et al.* 1997), and saturated within ~5 min (Figs 1*A* and 3*D*). The swelling-activated current had outwardly rectifying *I–V* characteristics (Fig. 1*B*). The changes in its reversal potential (Fig. 2*A* and *B*) induced by altering the transmembrane Cl^- gradient indicated that the current was carried primarily by Cl^- ions, although small organic anions (aspartate, glutamate or gluconate), when present, could also contribute to the current with a permeability P_x ~0·1 P_{Cl}. Furthermore, the known Cl^- channel blockers, 4,4′-diisothiocyanatostilbene-2,2-disulphonic acid (DIDS, 100 μM) and 5-nitro-2-(3-phenylpropylamino)benzoic acid (NPPB, 100 μM), both effectively inhibited the current (P. Doroshenko, unpublished observations). Thus, the volume-sensitive Cl^- channels in L-fibroblasts are similar in their basic biophysical properties to volume-sensitive Cl^- channels described in other mammalian cells (see reviews by Strange *et al.* 1996; Nilius *et al.* 1996; Okada, 1997).

The amplitude of the swelling-induced currents increased with a rise in either extracellular or intracellular Cl^- concentration, as expected from the electrodiffusion theory. When the extracellular Cl^- concentration was kept constant, a decrease in the intracellular Cl^- concentration selectively decreased the inward component of the transmembrane current (Fig. 2*A* and *B*), leaving its outward component largely unchanged. That could only happen if the maximal number of the Cl^- channels opened by the hyposmotic swelling was the same in the low-Cl^- and the high-Cl^- cells. These observations suggest that the maximal volume-sensitive conductance changed in accordance with the availability of the charge carriers (Fig. 2*C*) and that there was no modulatory action of the intracellular Cl^- ions on the maximal size of the conductance.

Cell volume and the volume-sensitive Cl^- conductance in patched cells

Given the unpredictability of hyposmotic swelling of patched cells discussed above, the lack of correlation between the extent of cell volume increase and the amplitude of the volume-sensitive Cl^- conductance in patched cells (Fig. 1*D*) is not surprising. A similar conclusion can also be drawn from the experiments shown in Figs 3 and 4. In the high-Cl^- cells activation of the swelling-induced conductance lagged behind volume changes by more than a minute (Fig. 4*A*), similar to what has been observed in lymphocytes (Ross *et al.* 1994), which is in agreement with the expected behaviour. In contrast, in the low-Cl^- cells the conductance increased faster and saturated before the cell volume had reached its maximal level, irrespective of the nature of the replacement anions: aspartate, glutamate or gluconate (Fig. 4*B–D*). It is likely that this phenomenon resulted from the use of the whole-cell recording mode. In patched cells the increase in cell volume during hyposmotic swelling was not only much larger than in intact cells but was also considerably prolonged (Fig. 1*C*). In intact cells the initial phase of hyposmotic swelling occurred quickly (Fig. 1*C*) and was large enough to reach the postulated threshold volume (e.g. in giardial cells at 106% of isosmotic volume; Park *et al.* 1998) at which the transition of the volume-sensitive Cl^- channels from the 'resting' to the 'open' state would occur.

Hence, in intact cells the activation of swelling-induced conductance will always be delayed in relation to cell volume increase. In patched cells, however, the apparent temporal relationship between the two processes can be unconventional under particular experimental conditions, e.g. in this study, at the low intracellular Cl^- concentration. It took ~5 min for the volume of the low-Cl^- cells to reach a saturating level during hyposmotic application (Fig. 3*C*, curve 1). It seems, therefore, that once triggered by a threshold increase in cell volume during hyposmotic swelling, the activation of the volume-sensitive Cl^- conductance was no longer linked to cell volume.

Cytosolic Cl^- ions affect the rate of activation of the volume-sensitive Cl^- conductance

The results of this study demonstrate that the rates of activation of the volume-sensitive conductance were definitely different in cells dialysed with solutions containing different concentrations of Cl^- ions. It was seen in hyposmotically swollen cells (Figs 3*D* and 4) and in inflated cells (Fig. 5). The main kinetic effect of raising the intracellular Cl^- concentration from 16 to 130 mM was a ~1·0 min increase in the half-activation time of the conductance. It seems unlikely that the delay was due to the larger conductance in the high-Cl^- cells, since the maximal number of open Cl^- channels was arguably the same in the low-Cl^- and high-Cl^- cells swollen by the same hyposmotic shift (see above).

The mechanism of this action of intracellular Cl^- ions is not clear. A similar delay in activation of the volume-sensitive conductance in patched C6 glioma cells, caused by elevation of the intracellular Cl^- concentration, has been attributed to a Cl^--dependent change in the volume set point (Emma *et al.* 1997). This argument, however, seems less applicable to inflated cells, where the volume set point should have been reached within a very short time both in the low-Cl^- and in high-Cl^- cells. Still, the half-activation time for the volume-sensitive conductance in the inflated high-Cl^- cells was ~0·7 min longer than in the inflated low-Cl^- cells (Fig. 5). To accommodate these observations, one has to assume that the cytoplasmic transduction processes (Hoffman & Dunham, 1995; Okada, 1997), linking an increase in cell volume to the opening of the volume-sensitive Cl^- channels, proceed more slowly at the higher cytoplasmic concentration of Cl^- ions. Available experimental observations show that intracellular Cl^- ions can affect a wide variety of signalling pathways, e.g. the G-protein-mediated activation of K^+ channels in heart atrial cells (Nakajima *et al.* 1992) and a putative protein kinase and/or phosphatase that is sensitive to the level of $[Cl^-]_i$ (see Treharne *et al.* 1994; Haas *et al.* 1995). Involvement of G-proteins (Doroshenko & Neher, 1992; Voets *et al.* 1998) and tyrosine phosphorylation (Doroshenko, 1998; Voets *et al.* 1998) in activation of volume-sensitive Cl^- currents in bovine chromaffin and pulmonary artery endothelial cells has been recently demonstrated.

In summary, these results show that during hypotonic swelling of patched cells the amplitude of the volume-sensitive Cl^- conductance is not related to the actual degree of cellular swelling and that the rate of its activation is dependent on the intracellular Cl^- concentration.

Churchwell, K. B., Wright, S. H., Emma, F., Rosenberg, P. A. & Strange, K. (1996). NMDA receptor activation inhibits neuronal volume regulation after swelling induced by veratridine-stimulated Na^+ influx in rat cortical cultures. *Journal of Neuroscience* **16**, 7447–7457.

Crowe, W. E., Altamirano, J., Huerto, L. & Alvarez-Leefmans, F. J. (1995). Volume changes in single N1E-115 neuroblastoma cells measured with a fluorescent probe. *Neuroscience* **69**, 283–296.

Doroshenko, P. (1998). Pervanadate inhibits volume-sensitive chloride current in bovine chromaffin cells. *Pflügers Archiv* **435**, 303–309.

Doroshenko, P. & Neher, E. (1992). Volume-sensitive chloride conductance in bovine chromaffin cell membrane. *Journal of Physiology* **449**, 197–218.

Du, X.-Y. & Sorota, S. (1997). Cardiac swelling-induced chloride current depolarizes canine atrial myocytes. *American Journal of Physiology* **272**, H1904–1916.

Ebihara, S., Shirato, K., Harata, N. & Akaike, N. (1995). Gramicidin-perforated patch recording: GABA response in mammalian neurones with intact intracellular chloride. *Journal of Physiology* **484**, 77–86.

Emma, F., McManus, M. & Strange, K. (1997). Intracellular electrolytes regulate the volume set point of the organic osmolyte/anion channel VSOAC. *American Journal of Physiology* **272**, C1766–1775.

Engstrom, K. G. & Savendahl, L. (1995). Cell volume and shape oscillations in rat type-II somatotrophs at hypotonic conditions. *Cytometry* **20**, 7–13.

Farinas, J., Simanek, V. & Verkman, A. S. (1995). Cell volume measured by total internal reflection microfluorimetry: application to water and solute transport in cells transfected with water channel homologs. *Biophysical Journal* **68**, 1613–1620.

Haas, M., McBrayer, D. & Lytle, C. (1995). $[Cl^-]_i$-dependent phosphorylation of the Na–K–Cl cotransport protein of dog tracheal epithelial cells. *Journal of Biological Chemistry* **270**, 28955–28961.

Hagiwara, N., Masuda, H., Shoda, M. & Irisawa, H. (1992). Stretch-activated anion currents of rabbit cardiac myocytes. *Journal of Physiology* **456**, 285–302.

Hamill, O. P., Marty, A., Neher, E., Sakmann, B. & Sigworth, F. (1981). Improved patch-clamp techniques for high-resolution current recording from cells and cell-free membrane patches. *Pflügers Archiv* **391**, 85–100.

Hoffmann, E. K. & Dunham, P. B. (1995). Membrane mechanisms and intracellular signalling in cell volume regulation. *International Review of Cytology* **161**, 173–262.

Hoffmann, E. K. & Simonsen, L. O. (1989). Membrane mechanisms in volume and pH regulation. *Physiological Reviews* **69**, 315–382.

Jackson, P. S., Churchwell, K., Ballatori, N., Boyer, J. L. & Strange, K. (1996). Swelling-activated anion conductance in skate hepatocytes: regulation by cell Cl^- and ATP. *American Journal of Physiology* **270**, C57–66.

Kubo, M. & Okada, Y. (1992). Volume-regulatory Cl^- channel currents in cultured human epithelial cells. *Journal of Physiology* **456**, 351–371.

Lenz, R. A., Pitler, T. A. & Alger, B. E. (1997). High intracellular Cl^- concentrations depress G-protein-modulated ionic conductances. *Journal of Neuroscience* **17**, 6133–6141.

Lewis, R. S., Ross, P. E. & Cahalan, M. D. (1993). Chloride channels activated by osmotic stress in T lymphocytes. *Journal of General Physiology* **101**, 801–826.

McCann, J. D., Li, M. & Welsh, M. J. (1989). Identification and regulation of whole-cell chloride currents in airway epithelium. *Journal of General Physiology* **94**, 1015–1036.

Miwa, A., Ueda, K. & Okada, Y. (1997). Protein kinase C-independent correlation between P-glycoprotein expression and volume-sensitivity of Cl^- channel. *Journal of Membrane Biology* **157**, 63–69.

Nakajima, T., Sugimoto, T. & Kurachi, Y. (1992). Effects of anions on the G protein-mediated activation of the muscarinic K^+ channel in the cardiac atrial cell membrane. Intracellular chloride inhibition of the GTPase activity of G_k. *Journal of General Physiology* **99**, 665–682.

Neher, E. (1992). Correction for liquid junction potentials in patch clamp experiments. *Methods in Enzymology* **207**, 123–131.

Nilius, B., Eggermont, J., Voets, T. & Droogmans, G. (1996). Volume-activated Cl^- channels. *General Pharmacology* **27**, 1131–1140.

Nilius, B., Sehrer, J., Viana, F., DeGreef, C., Raeymaekers, L., Eggermont, J. & Droogmans, G. (1994). Volume-activated Cl^- currents in different mammalian nonexcitable cell types. *Pflügers Archiv* **428**, 364–371.

Okada, Y. (1997). Volume expansion-sensing outward-rectifier Cl^- channel: fresh start to the molecular identity and volume sensor. *American Journal of Physiology* **273**, C755–789.

Park, J.-H., Edwards, M. R. & Schofield, P. J. (1998). Swelling detection for volume regulation in the primitive eukaryote *Giardia intestinalis*: a common feature of volume detection in present-day eukaryotes. *FASEB Journal* **12**, 571–579.

Robertson, M. A. & Fosket, J. K. (1994). Membrane crosstalk in secretory epithelial cells mediated by intracellular chloride concentration. *Japanese Journal of Physiology* **44** (suppl. 2), S309–S315.

Ross, P. E., Garber, S. S. & Cahalan, M. D. (1994). Membrane chloride conductance and capacitance in Jurkat T lymphocytes during osmotic swelling. *Biophysical Journal* **66**, 169–178.

Sakaguchi, M., Matsuura, H. & Ehara, T. (1997). Swelling-induced Cl^- current in guinea-pig atrial myocytes: inhibition by glibenclamide. *Journal of Physiology* **505**, 41–52.

Sorota, S. (1992). Swelling-induced chloride sensitive current in canine atrial cells revealed by whole-cell patch-clamp method. *Circulation Research* **70**, 679–687.

Stoddard, J. S., Steinbach, J. H. & Simchowitz, L. (1993). Whole cell Cl^- currents in human neutrophils induced by cell swelling. *American Journal of Physiology* **265**, C156–165.

Strange, K., Emma, F. & Jackson, P. S. (1996). Cellular and molecular physiology of volume-activated anion channels. *American Journal of Physiology* **270**, C711–730.

Treharne, K. J., Marshall, L. J. & Mehta, A. (1994). A novel chloride-dependent GTP-utilizing protein kinase in plasma membranes from human respiratory epithelium. *American Journal of Physiology* **267**, L592–601.

Voets, T., Manolopoulos, V., Eggermont, J., Ellory, C., Droogmans, G. & Nilius, B. (1998). Regulation of a swelling-activated chloride current in bovine endothelium by protein tyrosine phosphorylation and G proteins. *Journal of Physiology* **506**, 341–352.

Wang, X., Marunaka, Y., Fedorko, L., Dho, S., Fosket, J. K. & O'Brodovich, H. (1993). Activation of Cl^- currents by intracellular chloride in fibroblasts stably expressing the human cystic fibrosis transmembrane conductance regulator. *Canadian Journal of Physiology and Pharmacology* **71**, 645–649.

Worrell, R. T., Butt, A. G., Cliff, W. H. & Frizzell, R. A. (1989). A volume-sensitive chloride conductance in human colonic cell line T84. *American Journal of Physiology* **256**, C1111–1119.

Acknowledgements

I thank Dr Cathy Morris for commenting on this paper and David Mooney for reading it. Financial support was provided by the Medical Research Council of Canada and the Loeb Research Institute.

Correspondence

P. Doroshenko: Loeb Research Institute, 725 Parkdale Avenue, Ottawa, Ontario, Canada K1Y 4E9.

Email: petrod@civich.ottawa.on.ca